Decay kinetics of the 408 nm emission band from Pb^{2+} centres in KI single crystals

1994 J. Phys.: Condens. Matter 6 293

(http://iopscience.iop.org/0953-8984/6/1/029)

J. Phys.: Condens. Matter 6 (1994) 293–300. Printed in the UK

Decay kinetics of the 408 nm emission band from Pb^{2+} centres in KI single crystals

E Mihokova, M Nikl, K Polak and K Nitsch
Institute of Physics, Cukrovarnicka 10, 16200 Prague, Czech Republic

Received 10 August 1993

Abstract. Measurements of the time-resolved intensity and decay kinetics of the 408 nm emission band for KI:Pb^{2+} in the 4.2–100 K temperature range are reported. Two fast components and one slow component are observed. The temperature dependences of three decay times are interpreted in the framework of a three-excited-state-level model including multiphonon processes between two radiative and underlying metastable levels. Non-radiative quenching is also included to fit the decrease in overall intensity in the temperature range investigated.

1. Introduction

The absorption and emission properties of Pb^{2+}-doped alkali halides have been reported many times (see, e.g., recent review in [1]). The results of decay kinetics studies of these systems have been published less frequently, however. The existence of two fast components and one slow component was confirmed for KBr:Pb^{2+} [2, 3] and later for KCl:Pb^{2+} and KI:Pb^{2+} [4]. A three-excited-state-level model describing the temperature dependence of three decay times observed in the decay of Pb^{2+} emission centres in KI:Pb^{2+} was used in [4], as far as we know for the first time, to describe the decay kinetics parameters. However, the values published for the KI:Pb^{2+} slow-component lifetime are more than one order of magnitude shorter than those for KCl:Pb^{2+}, although their value is derived from vibronic interaction of Pb^{2+} with T_{2g} and E_g lattice modes, which should not be very different for KCl or KI crystals. Furthermore the model used in [4] does not include the non-radiative quenching decrease in the overall intensity of 408 nm band even if it follows from the data given in [5] that it has decreased by less than 10% of its liquid-He-temperature value already at 100 K. Including two-phonon processes in the non-radiative rate between sublevels of the split radiative $^3T_{1u}^*$ level results in a much better fit of one fast-component lifetime temperature dependence but leaves unchanged the other dominant fast-component lifetime dependence containing about 80% of overall intensity of the fast components.

When we used the parameters reported for Pb^{2+} emission centres in KI:Pb^{2+} [4] to calculate the ratio of overall fast to slow components, we obtained a value about a tenth of that expected according to our results from time-resolved emission spectra measurements.

Because of all these discrepancies we performed detailed decay kinetics measurements of the 408 nm emission band in KI:Pb^{2+} in the 4.2–100 K temperature range. We also measured the temperature dependence of the steady-state and time-resolved spectra in order to calculate the above-mentioned ratio. Furthermore the ratio of the two fast-component intensities was reconstructed from the fit of the fast-component decay curves to obtain a sufficient set of experimental data for unambigious determination of all the parameters of the theoretical three-excited-state-level model.

0953-8984/94/010293+08$07.50

2. Experimental details

Single KI:Pb^{2+} crystals were prepared at the Institute of Physics, Prague, by the Kyropoulos method in an argon atmosphere. Pb^{2+} ions were introduced by adding either $KPbI_3.2H_2O$ or $PbCl_2$ at several concentrations from several parts per million up to a few tenths of a part per million. No serious discrepancies were found between the different samples just described.

An Edinburgh Instrument 199S spectrofluorometer modified for low-temperature measurements was used for measurements of the decay kinetics and spectra. A nanosecond thyratron-gated flashlamp (FWHM 1.5 ns) [6] was used for measurements of the fast-component decay curves. The deconvolution procedure used in the evaluation procedure allows us to obtain even subnanosecond decay times with reasonable precision. A powerful microsecond xenon flashlamp (FX108AU; FWHM, 1–3 μs) excitation in the case of the slow-component measurements in connection with multiple accumulation of the decay curve in multichannel analyser of the 199S in scaling mode allows us to measure the slow-component decay with a good signal-to-noise ratio.

3. Experimental results

As we have already pointed out [7], in the case of KBr:Pb^{2+}, the decay of the slow component excited in the A absorption band deviates from a single exponential in its initial part and excitation in the B or C absorption band is more appropriate for obtaining true decay time values. This phenomenon is even stronger in the case of KI:Pb^{2+}, so that we measured the slow-component decay curves under B-band excitation (figure 1). The temperature dependences of the two fast-component and the slow-component lifetimes are given in figure 2.

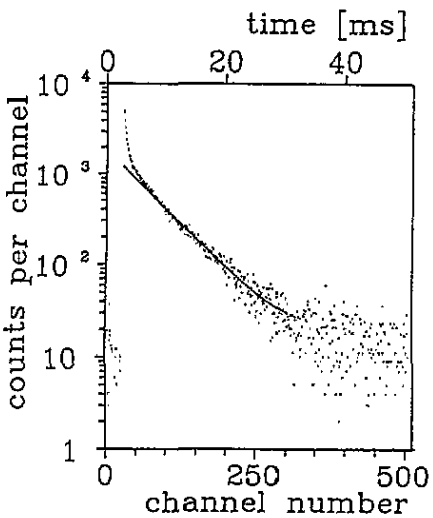

Figure 1. Slow-component decay of 408 nm emission in KI:Pb^{2+} at 4.2 K and excitation in the B absorption band (290 nm): ——, single-exponential approximation with the decay time $\tau = 7$ ms.

Furthermore we measured two different types of emission spectrum under the same excitation conditions with nanosecond flashlamp excitation.

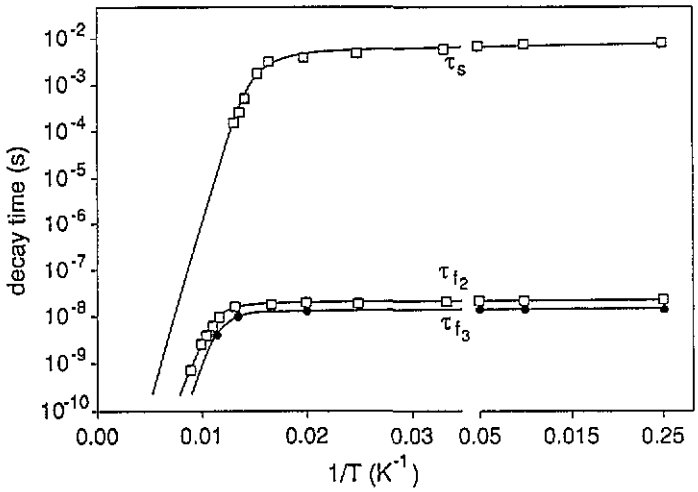

Figure 2. Temperature dependences of the slow-component decay time τ_s and two fast-component decay times τ_{f_2} and τ_{f_3} of 408 nm emission in KI:Pb^{2+} : ——, model sketched in figure 6(*a*) with parameters given in table 1.

Table 1. Parameters for three-excited-state-level model for 408 nm emission in KI:Pb^{2+}.

$k_1 = 133\ s^{-1}$
$k_2 = 4.41 \times 10^7\ s^{-1}$
$k_3 = 6.63 \times 10^7\ s^{-1}$
$K = 1.94 \times 10^6\ s^{-1}$
$K' = 1.4 \times 10^6\ s^{-1}$
$D = 55$ meV
$2E = 1.3$ meV
$p = 5$
$\hbar\Omega = 7$ meV
Initial populations
$n_{20}/n_{10} = 10^5$
$n_{30}/n_{20} = 0.23$
Quenching from levels
Level 1: $K_{1x} = 7 \times 10^{13}\ s^{-1}$, $\Delta E_{1x} = 155$ meV
Level 2: $K_{2x} = 4 \times 10^{13}\ s^{-1}$, $\Delta E_{2x} = 99$ meV
Level 3: $K_{3x} = 4 \times 10^{14}\ s^{-1}$, $\Delta E_{3x} = 110$ meV

(*a*) All emission photons were detected as in the case of steady-state excitation.

(*b*) Only photons from the overall fast component were detected (0–200 ns time gate related to the excitation pulse).

The area A under the spectra, which represents their integral intensity was then used to construct the ratio of the overall fast-component intensity to the slow-component intensity (figure 3):

$$I_f/I_s = A_{fast}/(A_{overall} - A_{fast}). \tag{1}$$

We also calculated the ratio I_{f_3}/I_{f_2} of the two fast-component intensities (see sketch of the model in figure 6(*a*)) using the two-exponential fit of the fast-component decay:

$I(t) = A_2 \exp(-t/\tau_{f_2}) + A_3 \exp(-t/\tau_{f_3})$ where τ_{f_2} and τ_{f_3} are the decay times from radiative levels 2 and 3 (figure 4):

$$I_{f_3}/I_{f_2} = A_3\tau_{f_3}/A_2\tau_{f_2}. \tag{2}$$

The temperature dependences of (1) and (2) and also of the overall emission $I(T)$ (figure 5) were used subsequently in addition to the decay time temperature dependences obtained in the model calculations described in the next section.

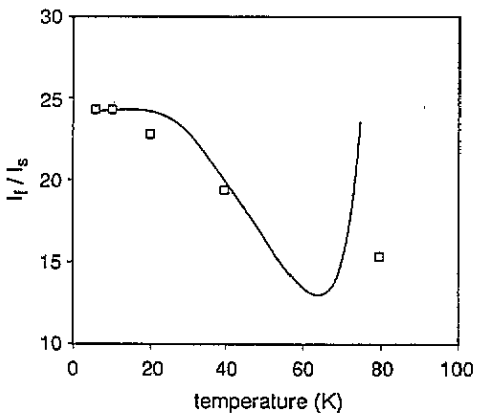

Figure 3. The temperature dependence of the overall ratio of the fast-component intensity to the slow-component intensity of 408 nm emission in KI:Pb^{2+}: ——, model sketched in figure 6(*b*) with parameters in table 1.

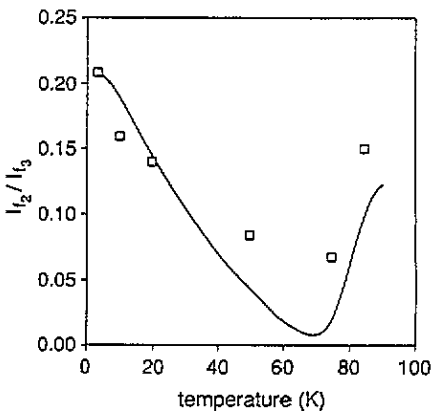

Figure 4. Temperature dependence of the ratio of the two fast-component intensities of 408 nm emission in KI:Pb^{2+}: ——, model sketched in figure 6(*b*) with parameters in table 1.

4. Theory

To explain the experimental data obtained, a simple kinetic model based on the three-level energy scheme as outlined in [4] was used (figure 6(*a*)). As mentioned above, experimental measurements of the luminescence decay show one slow component and two fast components. The slow-component decay time τ_s is due to the emission from the $^3A_{1u}$ trap level 1 while the two fast-component decay times τ_{f_2} and τ_{f_3} are due to radiative transitions from levels 2 and 3. The definition of the parameters is shown in figure 6(*a*).

We assumed multiphonon non-radiative processes between the radiative levels and the metastable level as in [8, 9] and one-phonon processes between the two radiative levels. Hence

$$k_n = K(n+1)^p \qquad k'_n = Kn^p \tag{3}$$

where p is the number of photons included in the process and

$$k_{32} = K'(n'+1) \qquad k_{23} = K'n' \tag{4}$$

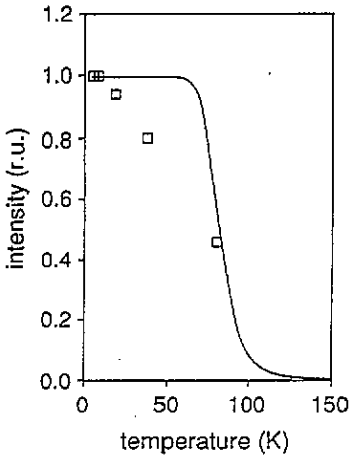

Figure 5. Temperature dependence of the overall 408 nm emission intensity for KI:Pb^{2+}: ——, model sketched in figure 6(*b*) with parameters in table 1.

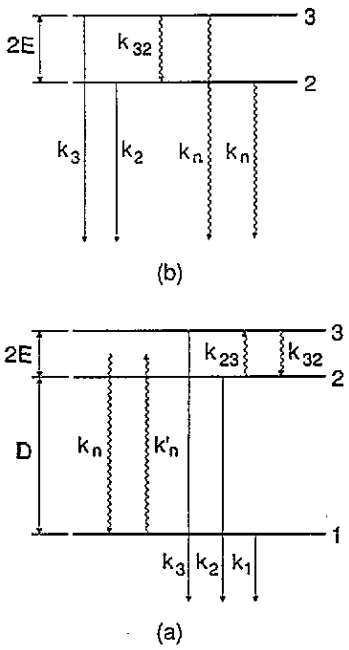

Figure 6. (*a*) The energy level scheme used for interpretation of the decay kinetics and time-resolved emission spectra of the 408 nm emission of KI:Pb^{2+}. (*b*) The same energy level scheme as in (*a*) in the low-temperature limit.

with

$$n = [\exp(D/k_B T) - 1]^{-1}$$
$$n' = [\exp(2E/k_B T) - 1]^{-1}. \tag{5}$$

The rate equations for the populations N_i of the $i = 1, 2, 3$ levels are given by the matrix expression

$$\frac{\mathrm{d}}{\mathrm{d}t}\begin{pmatrix} N_1 \\ N_2 \\ N_3 \end{pmatrix} = \begin{pmatrix} s & -k_n & -k_n \\ -k_n & q & -k_{32} \\ -k_n & -k_{23} & r \end{pmatrix}\begin{pmatrix} N_1 \\ N_2 \\ N_3 \end{pmatrix} \tag{6}$$

where $s = k_1 + 2k'_n$, $q = k_2 + k_n + k_{23}$ and $r = k_3 + k_n + k_{32}$. The total emission can be represented by the superposition of three exponential decays:

$$N_i = \sum_j A_j \exp(-t/\tau_j). \tag{7}$$

The three inverse decay times τ_j^{-1} are given by the eigenvalues of the matrix of the coefficients in equation (6).

In the low-temperature limit $T \to 0$ of the model when the inverse non-radiative transition parameters k'_n and k_{23} are negligible, one can find that

$$1/\tau_s \to k_1 \tag{8}$$

$$1/\tau_{f_2} \rightarrow k_2 + K \tag{9}$$

$$1/\tau_{f_3} \rightarrow k_3 + K + K'. \tag{10}$$

From equation (8) we immediately have the value of k_1. To establish the values of k_2 and K, consider the following: at 4.2 K we have measured the value of the ratio $I_{f_3}/I_{f_2} = 0.21$ of the fast-component intensities. This shows that the dominant contribution to the total fast-component intensity $I_f = I_{f_2} + I_{f_3}$ comes from level 2 (at liquid-He temperature) and that is why it might be reasonable to use the approximation of the two-level model (with one radiative level and one metastable level usable for monovalent dopants) when the ratio I_f/I_s of the fast-component intensity to the slow-component intensity is concerned. In this limit under the condition $n_{10} = 0$ for the initial population of the level 1, one has [10]

$$I_f/I_s = k_2/K. \tag{11}$$

From (9) and (11) we found the values of k_2 and K. From the condition (10) the temperature dependence of the fast-component decay time τ_{f_3} in the region 4.2–70 K and the temperature course of I_{f_3}/I_{f_2} as well, we obtained the values of k_3 and K' using the value of the energy splitting $2E$ from [4].

We can find the ratio N_{30}/N_{20} of the two upper-level initial populations from the low-temperature limit of the ratio I_{f_3}/I_{f_2} of the fast-component intensities. When we are looking for this limit we can use the model in figure 6(*a*) as a two-level model, as level 1 does not contribute to the fast-component intensities in the low-temperature limit (see figure 6(*b*)). Such a system is described by rate equations of the form

$$\frac{\mathrm{d}}{\mathrm{d}t}\begin{pmatrix} N_2 \\ N_3 \end{pmatrix} = \begin{pmatrix} (-k_2 + K) & K' \\ 0 & -(k_3 + K' + K) \end{pmatrix}\begin{pmatrix} N_2 \\ N_3 \end{pmatrix}. \tag{12}$$

Solving the system, one obtains

$$N_3^0/N_2^0 = (I_{f_3}^L/I_{f_2}^L)(\tau_{f_2}^L k_2/\tau_{f_3}^L k_3) \tag{13}$$

where $I_{f_3}^L$, $I_{f_2}^L$ and $\tau_{f_2}^L$, $\tau_{f_3}^L$ are the fast-component intensities and fast-component decay times respectively in the low-temperature limit.

We obtained the value of the energy difference D between levels 1 and 2 from the best fit of τ_s in the temperature range 50–70 K as well as the temperature dependence of I_f/I_s. To determine the slight low-temperature dependence of τ_s we considered the temperature dependence of k_1 expressed in the formula

$$k_1(T) = k_1(0)\coth(\hbar\Omega/2kT) \tag{14}$$

as in [8] with the energy $\hbar\Omega = 7$ meV.

As luminescence quenches at temperatures even below 100 K the number of phonons involved in the non-radiative processes between levels 1 and 2 could not be found from the high-temperature course of the fast-component decay times as, for example, in the cases of KCl:Tl^+ [8] or KBr:Tl [10], for the influence of quenching in this region is dominant. Instead we used the best fit of I_f/I_s the temperature dependence of which is controlled in particular by the values of p and D.

Finally from the high-temperature dependence of all the decay times we obtained the parameters of the quenching channels that have the form

$$k_{ix} = K_{ix}\exp(-\Delta E_{ix}/k_B T) \qquad i = 1, 2, 3 \tag{15}$$

where ΔE_{ix} can be interpreted as the height of the barrier between the minima of the corresponding excited states i and the ground state or the X minima [5].

The list of calculated parameters is given in table 1.

5. Discussion

The aim of the rough description of our evaluation strategy given above was to point out the importance of a sufficiently large experimental data set in order to determine all the parameters of the model sketched in figure 2 as unambiguously as possible. Even if we do not include the non-radiative quenching channels (which is apparently wrong; see steady state intensity temperature dependence in figure 5), we have to determine at least ten independent parameters, and, for their unambiguous determination, knowledge of only the experimentally obtained values of the decay times is not sufficient.

While the agreement between the experimental temperature dependence of decay times and the model calculations in figure 2 is very good, in the case of the time-resolved spectra and the steady-state intensity temperature dependences in figures 3–5 it is not perfect. There are basically two reasons for this.

(i) The slow component above 30 K becomes very weak; when one constructs the ratio (1), two close numbers in the denominator are subtracted and the error in the result is therefore increased (figure 3).

(ii) The two-exponential fit of the fast component-decay is given by two relatively close decay times (21.5 ns and 14.4 ns at 4.2 K) and to find the best parameters for the fit in the least-squares sum fitting procedure requires rather good resolution and a large dynamic range of the measured decay curves. In particular the values of the decay time τ_{f_3} belonging to level 3 are at $T > 40$ K very sensitive even to a small variation (less than 5%) in the decay time τ_{f_2}, which strongly influences the calculated values in figure 4.

It is impossible to fit a gradual decrease in the overall steady-state intensity between 20 and 70 K in figure 5 in a better way. Probably another mechanism not included in our model plays a significant role at these temperatures. Because of the relatively small absorption of the samples in the A absorption band of Pb^{2+} (about 30–50% of the excitation light passes through the sample) any change in the absorption coefficient at the excitation wavelength with increasing temperature results in a change in the observed emission intensity. The known behaviour of the temperature dependence of the A absorption band of Pb^{2+} in alkali halides (decrease in the absorption maximum with increasing temperature) could provide a partial explanation. The other reason could be connected with the rather complex structure of the excited state of Pb^{2+} [5], where tunnelling of the energy between the equivalent minima occurs at $T > 30$ K, which could result in the different spatial distribution of the emitted light and a possible decrease in the intensity in the direction of the detection photomultiplier.

In connection with the observed splitting of the minima of RES (the X and Y minima are lower than the Z minimum) [5] it is possible to consider also a rather different hypothesis to explain the presence of two fast components in the decay of KI:Pb^{2+}. One could ascribe one fast component to the emission from thermalized levels 2 and 3 from the Z minimum and the other as arising from the X and Y minima; for both kinds of minimum, one can apply the same scheme as drawn in figure 6 (for such a case, two slow luminescent components would also be expected). However, because of the unusual behaviour of the initial part of the slow component obtained experimentally, one cannot decompose it simply into two exponentials one of which originates from the X and Y minima and the other from the Z minimum). The splitting of levels 2 and 3 is very small with respect to the energy separation from the higher-lying $^1T_{1u}$ level, which, because of spin–orbit coupling, is responsible for the rather 'allowed character' of transitions from these levels to the ground state. That is, it is reasonable to assume very close values of k_2 and k_3 and thermalization between levels 2

and 3 even at 4.2 K, which could result in the observation of one fast component from the X and Y minima and a second fast component from the Z minimum. Of course, if such a hypothesis is confirmed, a different interpretation of, for example, I_{f_3}/I_{f_2} would need to be given. A trial to change the ratio of the intensities of fast components in the decay using polarizers in the excitation and emission beams could serve as a test of this hypothesis. It is reasonable to suppose that, while the emission coming from levels 2 and 3 from a single minimum has the same polarization properties, different polarizations of the components could be expected when they come from different minima. However, as the positions of the vacancy and Pb^{2+} ion have no preferential direction with respect to the coordinate system connected with the crystal (and the experimental set-up), it is hard to predict whether and in which way the introduction of polarizers could influence the detected decay curve and the ratio of the two fast components. Because of this uncertainty we utilized the model given in [4] as a starting point in the analysis and left the above-given hypothesis open for future discussion.

Acknowledgment

The authors are grateful to V Nagirnyi from the Institute of Physics, Tartu, Estonia, for valuable discussions.

References

[1] Jacobs P W M 1991 *J. Phys. Chem. Solids* **52** 35
[2] Schmitt K, Sivasankar V S and Jacobs P W M 1982 *J. Lumin* **27** 313
[3] Kang, J G, Belliveau T F and Simkin D J 1983 *Chem. Phys. Lett.* **101** 381
[4] Kang, J G, Cusso, F, Belliveau T F and Simkin D J 1985 *J. Phys. C: Solid State Phys.* **18** 4753
[5] Nagirnyi V, Nikl M, Polák K, Zazubovich S and Jaanson N 1993 *Phys. Status Solidi* b **178** 173
[6] Birch D J S and Imhof R E 1977 *J. Phys. E: Sci. Instrum.* **10** 1044
[7] Polák K, Nikl M and Mihoková E 1992 *J. Lumin.* **54** 189
[8] Hlinka J, Mihóková E, Polák K and Nikl M 1991 *Phys. Status Solidi* b **166** 503
[9] Nikl M, Mihóková E, Polák K, Fabeni P and Pazzi G P 1993 *Phil. Mag.* B **67** 627
[10] Hlinka J, Mihóková E, Nikl M, Polák K and Rosa J 1993 *Phys. Status Solidi* b **175** 523